



Independent component analysis using prior information for signal detection in a functional imaging system of the retina

E. Simon Barriga^{a,b,*}, Marios Pattichis^a, Dan Ts'o^c, Michael Abramoff^d, Randy Kardon^d, Young Kwon^d, Peter Soliz^{b,d}

^a University of New Mexico, Electrical and Computer Engineering Department, Albuquerque, NM, United States

^b VisionQuest Biomedical., Albuquerque, NM, United States

^c SUNY Upstate Medical University, Syracuse, NY, United States

^d University of Iowa, Department of Ophthalmology and Visual Sciences, Iowa City, IA, United States

ARTICLE INFO

Article history:

Received 27 December 2008

Received in revised form 9 May 2010

Accepted 21 June 2010

Available online 6 July 2010

Keywords:

Independent component analysis

Functional imaging

Retina

Visual stimulation

ABSTRACT

Independent component analysis (ICA) is a statistical technique that estimates a set of sources mixed by an unknown mixing matrix using only a set of observations. For this purpose, the only assumption is that the sources are statistically independent. In many applications, some information about the nature of the unknown signals is available. In this paper we show a method for incorporating prior information about the mixing matrix to increase the levels of detection of responses to visual stimuli. Experimentally, our method matches the performance of known ICA algorithms for high SNR and can greatly improve the performance for low levels of SNR or low levels of signal-to-background ratio (SBR). For the problem of signal extraction, we have achieved detection for signals as small as 0.01% (−40 dB SBR) in hybrid live/synthetic data simulations. In experiments using a functional imager of the retina, measured changes in reflectance in response to visual stimulus are in the order of 0.1–1% of the total pixel intensity value, which makes the functional signal difficult to detect by standard methods. The results of the analysis show that using ICA-P signal levels of 0.1% can be detected.

The approach also generalizes the standard Infomax algorithm which can be thought of as a special case of ICA-P when the confidence parameter or a tolerance value is zero. For in vivo animal experiments, we show that signal detection agreement over a range of confidence values parameters can be used to establish reflectance changes in response to the visual stimulus.

© 2010 Elsevier B.V. All rights reserved.

1. Introduction

In a recent paper (Barriga et al., 2007), the application of Independent Component Analysis (ICA) in the detection of functional responses from retinal activation due to visual stimulus has been demonstrated. In this prior work, we quantified the values for detection of functional signal in presence of noise. From these earlier results we discovered a large decrease of performance at considerable levels of noise (10 dB SNR) or low levels of functional signal (−40 dB SBR). In this paper, we investigate the use of temporal prior information about the visual stimulus producing the functional signal to increase sensitivity of the method in the presence of high noise levels.

It has long been recognized that the retina's optical properties, when stimulated by visible light, are altered depending on what

part of the near infrared (NIR) spectrum is being used to measure the changes in reflectance (Ts'o et al., 2004, 2003; Hanazono et al., 2007; Hofmann et al., 1976; Tsunoda et al., 2004; Abramoff et al., 2006). A strategy to capture the signal from the stimulated retina was originally devised by two groups, including ourselves Kardon et al. (2002), Grinvald et al. (1986), and Nelson et al. (2005), that included image and signal processing techniques for extracting the intrinsic signal (Barriga et al., 2007). A number of proposed sources of this functional signal, including photoreceptors (Kahlert et al., 1990), membrane depolarization (Stepnoski et al., 1991), and altered metabolism have been attributed to the changes in the local optical properties of the retinal tissue that are detectable by measurement of light-scattering signals. In an effort to isolate the source of this signal, several ex vivo studies of retinal samples (Yao and George, 2006) have measured stimulus-induced intrinsic NIR signals that have been recorded from retinal layers, including the inner retina and the region of the optic disc (Ts'o et al., 2009).

In recent papers by our collaborators, Schallek et al. (2009a,b), as well as publications by others, Tsunoda et al. (2004), it has been

* Corresponding author at: University of New Mexico, Electrical and Computer Engineering Department, Albuquerque, NM, United States. Tel.: +1 505 507 2183; fax: +1 505 277 1439.

E-mail address: sbarriga@visionquest-bio.com (E.S. Barriga).

established that the intrinsic signal is likely to originate from the outer retina, i.e., the photoreceptors. Schallek et al. performed experiments to pharmacologically suppress activity in the inner retina with intravitreal injections of tetrodotoxin (TTX) to suppress the innermost retinal layers consisting of ganglion cells, their axons, and spiking amacrine cells (Hare and Ton, 2002) and injections of 2-amino-4-phosphonobutyric acid (APB) blocked photoreceptor input to the “ON” bipolar cells of the retina, while cis-2,3-Piperidinedi-carboxylic acid (PDA) suppressed the “OFF” bipolar cell response and cell types downstream from this pathway (Slaughter and Miller, 1983). When injected together, these drugs suppress the stimulus-evoked potential at the level of the bipolar cell input, while leaving photoreceptor function intact. The stimulus-evoked intrinsic signal was observed to be as strong under these conditions as under the control, non-pharmacologically altered state. This leads to the conclusion that the intrinsic signal is significantly driven by the photoreceptors stimulation.

The optical imaging device of retina function (OID-RF) has been developed in an attempt to improve the objectiveness of the test and the sensitivity for detection of damage and change over time. The OID-RF is based on early research by Hill and Keynes (1949), who linked the activity of the nerve cells with changes in their optical properties. Grinvald et al. (1986) showed that changes in the optical properties of the tissue could be used to study the functional architecture of the cortex. Villringer and Chance (1997) used near-infrared light to assess brain activity in humans non-invasively through the skull. Kardon et al. (2002) reported the first device to directly image the human retina by recording changes in 700 nm light caused by retinal activation in response to a 535 nm stimulus. The authors of this paper have reported on an optical imaging device of retina function (OID-RF) that has been developed to improve the objectiveness and sensitivity of visual testing (Kardon et al., 2002; Abramoff et al., 2006; Barriga et al., 2007; Ts'o et al., 2003).

These findings motivated the development of a functional imager of the retina that can, using an instrument suitable for the clinical environment, directly measure spatially resolved retina function. The OID-RF is a non-invasive imaging device that measures the increase or decrease in retinal reflectance due to changes in retinal metabolism thought to be a result of blood oxygen uptake and capillary response due to neural activity resulting from visual stimulation of the photoreceptors in the human retina. The functional measurements are stored as optical recordings (videos). The hypothesis is that a visual stimulus causes the retina to alter its level of blood volume and the ratio of oxygenated hemoglobin (HbO) to deoxygenated hemoglobin (Hb). This has the effect of altering the spectral reflectance characteristics of the retina and in turn results in a change in the reflected intensity of the image in the stimulated area.

In recent years, ICA has been applied to many biological related problems such as electroencephalography (EEG) data analysis (Makeig et al., 1996; Jung et al., 2000), and electrocardiogram (ECG) data analysis (Choi et al., 1999). Schiessl et al. (2000) and Stetter et al. (2000) applied ICA techniques to isolate changes on the brain cortex of a macaque monkey due to visual stimulation. ICA has also been used for motion correction in image sequences by maximizing spatial independence (Liao et al., 2005; Milles et al., 2008), and in perfusion sequence analysis (Juslin et al., 2005). ICA has been applied extensively to detect functional brain activation in functional magnetic resonance imaging (fMRI) experiments (McKeown and Sejnowski, 1998; Calhoun and Adali, 2006). Park et al. (2002) have applied ICA to model the role of the visual cortex to locate salient areas in an image. They found that ICA was useful in reducing the redundancy of data or signals from the retina to the visual cortex. They defined the signals based on traditional techniques which use color opponent coding and edge

detection to model the output from the retina. The authors of this paper have previously reported on the application of ICA techniques to isolate the changes produced in the retina due to visual stimulation (Barriga et al., 2003a, 2003b, 2006, 2007).

In this paper we demonstrate the application of ICA with priors and compare our results to standard ICA methods developed by Barriga et al. (2007) for a set of in vivo data collected in an animal study. The data was collected using the OID-RF instrument to extract the functional signal due to retinal stimulation. In our animal study, we expect the major contributors to the signals will be due to cardiac function, the respiratory cycle, and the evoked response. We note that these components correspond to independent physiological processes that should yield independent signals that are appropriate for ICA. In our ICA algorithm (ICA-P), we investigate the use of prior information about the temporal nature of the stimulus that produces the functional signal. The priors of the mixing matrix are modeled using information about the timing on which the visual stimulus was applied to the retina. We measure the performance of ICA-P on a set of two-dimensional spatiotemporal synthetic simulations and then apply it to data collected in in vivo cat experiments (Ts'o et al., 2003). We also compare the results of ICA-P with other well-established ICA algorithms, such as Infomax (Bell and Sejnowski, 1995) and JADE (Cardoso, 1997). We show that the use of prior information leads to significant improvements, such as allowing the detection of weak signals that are of 1% of the background noise.

This paper is organized as follows: Section 2 presents the ICA-P method used in the analysis of the synthetically-generated data and the live cat data. Section 3 describes the performance measurements and synthetic simulation methods used to validate the use of ICA-P in the data. Section 4 shows the results obtained by applying the ICA-P techniques in anesthetized cat data. Discussion of the results and conclusions are given in the last two sections.

2. Methods

2.1. Independent component analysis (ICA)

Let $X = [x_1(t)x_2(t) \cdots x_n(t)]$ be a vector of our observations, modeled as a collection of random processes. We assume that the observations are due to a linear mixture of signal components $S = [s_1(t)s_2(t) \cdots s_n(t)]$. If we let A denote the mixing matrix, then

$$X = AS \quad (1)$$

Then, using independent component analysis (ICA), we can estimate both A and S using only the observations X , assuming that the source signals are statistically independent (Hyvarinen et al., 2001). In neuroscience applications it has been previously demonstrated that by adding some knowledge about the experimental procedures to which an individual is subjected, we can increase signal detection. Particularly, in fMRI experiments, Calhoun et al. (2005) and Calhoun and Adali (2006) incorporated information about visual tasks as priors of the ICA mixing matrix. In their method, they constrain one or many of the components of the mixing matrix to be close to a paradigm-derived time course. Similarly, in this paper, we investigate the use of prior information of temporal characteristics of the visual stimulus.

2.2. ICA using priors

In our experimental procedures with retinal stimulation we know the onset and offset of the visual stimuli which indirectly gives us information about the mixing matrix. The Infomax algorithm (Bell and Sejnowski, 1995) is modified so that we incorporate prior information at each update cycle. In the classic cocktail

party problem for which ICA was originally developed, the temporal signals are considered to be the source signals, and spatial information is contained in the mixing matrix. For our problem, the spatial images are the source signals, which are combined temporally by the mixing matrix to form the resulting videos to be analyzed.

Prior information is incorporated in the estimated mixing matrix \hat{A} . The basic information that we want to incorporate is that the response signal will have to follow the stimulus signal. In what follows, let the i th signal represent the response signal. Starting from Eq. (1), we then have that the i th column of \hat{A} is filled with zeros before the response signal is expected to start, with ones for the period of stimulation, and zeros for the post-stimulation period. The rest of the columns are filled with zeros. We then calculate the estimate of the unmixing matrix $\hat{W} = \hat{A}^{-1}$ and use it to update the algorithm.

Starting from the Bell–Sejnowski form of the Infomax algorithm, the negative log-likelihood function for the unmixing matrix (W) is given by:

$$f(W) = -[N \log |W| - \sum_{ij} \cosh(WX) - NM \log(\pi)] \quad (2)$$

where N and M are the dimensions of the data (temporal and spatial data points), X is the vector of observations, and W is the estimated unmixing matrix, which is the inverse of the estimated mixing matrix (A). The gradient of the unmixing matrix is:

$$\Delta W = -[N(W^T)^{-1} - \tanh(WX)X^T] \quad (3)$$

Using the log-likelihood function and the gradient we can use an optimization method to obtain an estimate of the unmixing matrix. We used the BFGS method for unconstrained optimization. At each iteration, a normalized cross-correlation (absolute NCC) measure between the estimated mixing matrix and the prior of the mixing matrix is performed at zero lag. Then, the estimated mixing matrix is updated as:

$$W^i = \begin{cases} W^i, & \text{NCC} \geq t \\ W^i + c(W_p^i - W^i), & \text{NCC} < t. \end{cases} \quad (4)$$

where W^i is the i th column of the estimated mixing matrix, W_p^i is the prior for that column and c is a confidence value parameter (between 0 and 1) for the prior information. If the correlation is lower than a tolerance value t then the estimated unmixing matrix is updated using the priors and the confidence parameter. In the optimization algorithm, we then invert the updated version of the unmixing matrix to obtain an estimate of the mixing matrix.

The tolerance defines the threshold of uncorrelatedness between the estimated signal and the prior. If the NCC is lower than this threshold, the estimated is corrected using the prior. Here, we are not using the NCC to account for any lags between the stimulus and the response. All lags are incorporated in the priors. It is important to notice that we apply the prior to just one of the columns of the estimated mixing matrix, corresponding to one of the estimated signals, as we do not want to influence the estimation of the remaining components of the mixing matrix.

We note that for the cases when $c = 0$ or $t = 0$, we have the original Infomax algorithm. Thus, the proposed algorithm represents a generalization of the Infomax algorithm. The update in (4) can also be interpreted from an optimization perspective. Essentially, high values of NCC are used as an indication that the search for a minimum is proceeding in the right direction. On the other hand, low values for NCC are used to indicate that we may be at a local (not global) minimum.

2.3. Parameter values

We have experimented with a range of values for confidence and tolerance. We set up one-dimensional simulations to separate a small sigmoidal signal from sinusoids using a sigmoid as the prior. We selected these signals as an approximation of physiolog-

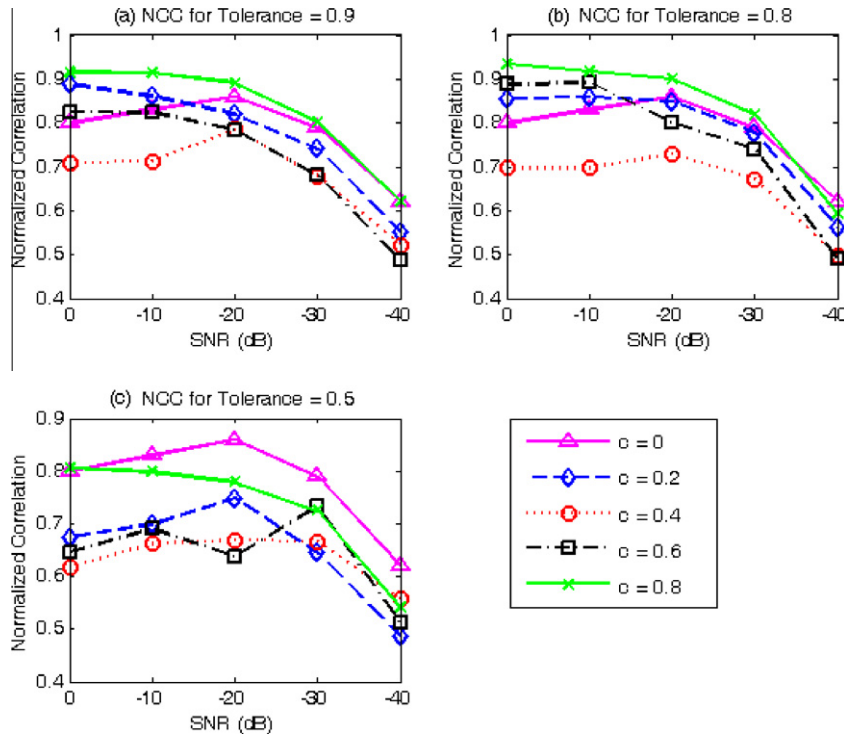


Fig. 1. NCC values for different tolerance and confidence values.

ical processes, such as the visual stimulus response, respiration, and cardiac cycles. See Barriga et al. (2007) for detailed descriptions of these signals.

Fig. 1 shows the normalized cross-correlation values between the estimated signal and the original source for different signal-to-noise ratios and for different confidence and tolerance parameters. As expected, NCC values decrease as the noise increases. Ideally, we want to use the parameters that give us high NCC at high levels of noise (low SNR).

An important observation from Fig. 1 is that for very low SNR values, we have the relative convergence of the NCC values over a wide range of values of the confidence parameter. We have observed this same behavior for detection in animal data. Thus, agreement for several confidence values maybe considered for helping to detect very weak signals. A high confidence value of 0.8 yields the best results over the majority of the noise levels. On the other hand, it is also interesting to note that the low confidence value of 0.2 also gave near optimal results for several SNR values, while intermediate values did not. For tolerance, we can see that $t = 0.8$ yields equal or better results as for the high value of $t = 0.9$. For a tolerance value of 0.5 we note that the original Info-max algorithm performs better than any of the ICA-P implementa-

tion, which makes us conclude that overall, the new method requires high confidence and high tolerance values for detecting existing signals in noise.

3. Performance measurements on synthetic data simulations

In the ICA literature there have been many efforts to quantify the performance of the algorithms. Most of these efforts are confined to one-dimensional data sets, with few focusing on 2-dimensional data and almost none on three-dimensional video applications. It is therefore very important to explore the performance of the selected ICA algorithms in realistic simulations of both general spatiotemporal data sets as well as more specific data sets that are constructed from actual optical imaging data from the OID-RF device (Kardon et al., 2002).

In this section, three different ICA methods are compared using three-dimensional data sets. The performance of the algorithms is tested under a range of signal-to-noise ratios (SNRs) using normalized cross-correlation with known sources. In these simulations, the sources have a temporal structure resembling some physiological processes observed during optical stimulation of the retina.

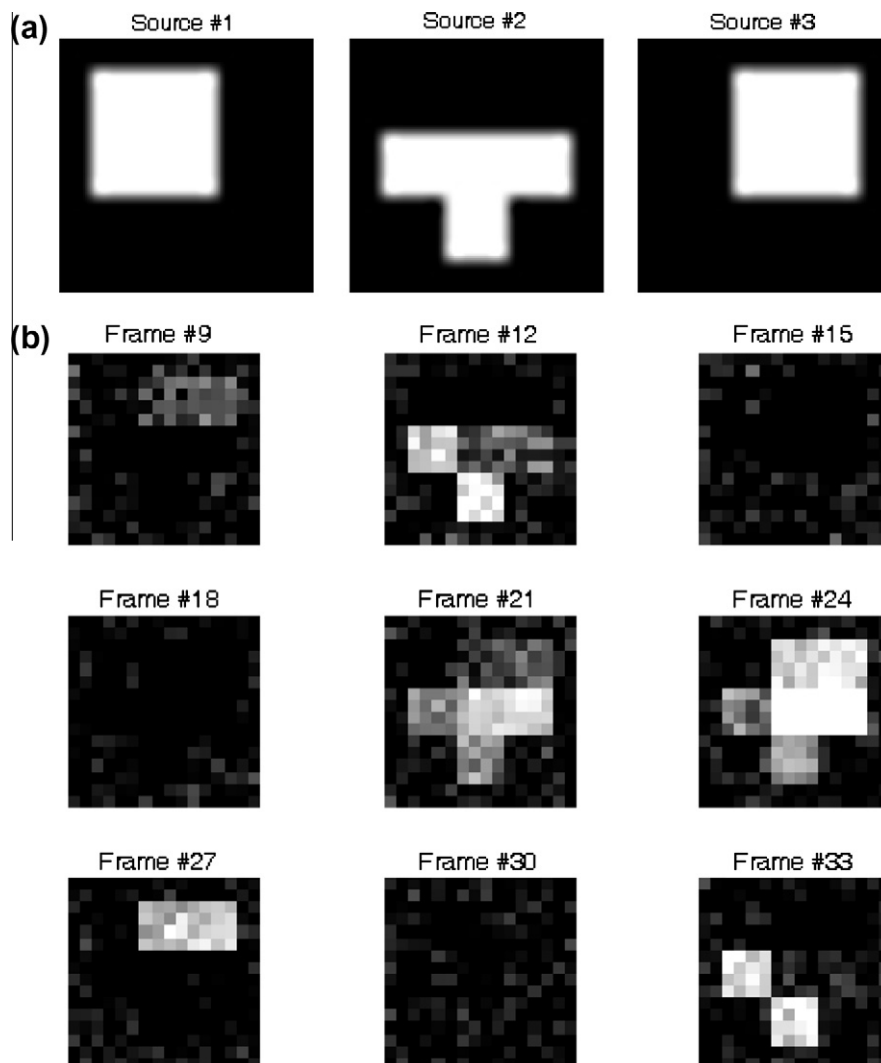


Fig. 2. (a) Unmixed spatial source signals. (b) Nine frames from a synthetic video simulation generated using sources above. Noise is added with SNR of 10 dB. Source #1 is the one affected by the sigmoid at 1% intensity, and it is not noticeable in the video.

3.1. Synthetic video simulation

For this simulation a video is generated by mixing three images (sources, Fig. 2a) with a mixing matrix that contains the temporal structures of two sinusoids and a smoothed step function. The setup of the experiment is as follows: Three source signals are mixed by a random mixing matrix. Noise is added at the determined level of SNR to produce the mixtures. Those mixtures are the input to the ICA algorithms. Fig. 2b shows sample frames of the generated video sequence. The resulting estimated sources are compared with the known sources to determine the accuracy of the estimated signal.

The temporal signals are described as:

- Sinusoid #1: Period is 20 samples, peak-to-peak amplitude is 2 (units are arbitrary).
- Sinusoid #2: Period is 10 samples, peak-to-peak amplitude is 2.
- Smoothed negative rectangular function: This function is formed as a union of two sigmoids and is intended to be a rudimentary model of a biological response to the stimulation. This signal can also be modified to simulate the BOLD response more accurately, but for the purposes of the experiments a simple approximation was chosen. The amplitude of this signal varies in three different experiments: 10%, 5%, and 1% of the peak-to-peak amplitude of the sources. The rectangular function is on from frame 10 until frame 30.

Gaussian noise is added to the mixture of signals with an SNR ranging from 40 dB to 0 dB. By calculating the variance of the original mixture we generate the appropriate noise level by varying its variance such that:

$$\text{SNR (dB)} = 10 \log_{10} \frac{\sigma_S^2}{\sigma_N^2} \quad (5)$$

where σ_S^2 is the variance of the original mixture and σ_N^2 is the variance of the Gaussian noise.

After applying all the ICA algorithms to this new mixture (the original video plus the noise), we compared the estimated sources and mixing matrix with the originals using the absolute NCC value

at zero lag. The sources comparison tells us how accurate the spatial localization is, whereas the mixing matrix comparison establishes the accuracy of the temporal reconstruction.

The results from the normalized cross-correlations between the estimated sources and estimated mixing matrices are shown in Fig. 3. The functional response is modeled as a step source with three different amplitudes, 10%, 5% and 1% of the total intensity of the images. We compare the results of ICA-P with the ones obtained using Infomax (Bell and Sejnowski, 1995) and JADE (Cardoso, 1997). The “temporal” results refer to the comparison of the columns of the mixing matrices while the “spatial” results refer to the comparison of the sources with their estimated counterparts.

Fig. 3 shows how ICA-P achieves NCC values close to 1 even for a low SNR. JADE matches the ICA performance for high SNR, but its NCC values drop as the signal intensity is reduced. We are particularly interested on the performance of the algorithms on the detection of the step function, as this represents the functional signal. From Fig. 3c, it is clear that ICA-P can be used to detect the temporal signal at 0 dB (NCC > 0.8 for SNR = 0 dB). Among the standard ICA algorithms, JADE performs the best. JADE can also detect this signal at levels of 30 dB or higher (see Fig. 3c). This suggests that ICA-P can detect the temporal signals at a 30 dB lower level than any of the other algorithms.

3.2. B. Live data with simulated visual stimulus

The next simulation involved the mixture of live cat data with a synthetic stimulation (see Barriga et al., 2007 for more details on the simulation setup). The live data comes from experiments performed by Ts'o et al. (2003). We use the OID-RF recordings from an unstimulated cat retina and add a synthetic stimuli at different levels of signal-to-background ratio (SBR). The synthetic stimuli are obtained from actual recordings of stimulated cat retina and synthesized so it can be easily manipulated in our simulation.

Using an unstimulated cat video as the baseline, the model of the functional response is added. Sample frames from the resulting video are presented in Fig. 4. The amplitude of functional response that is added to the baseline video is defined by its Stimulus-to-Background Ratio (SBR):

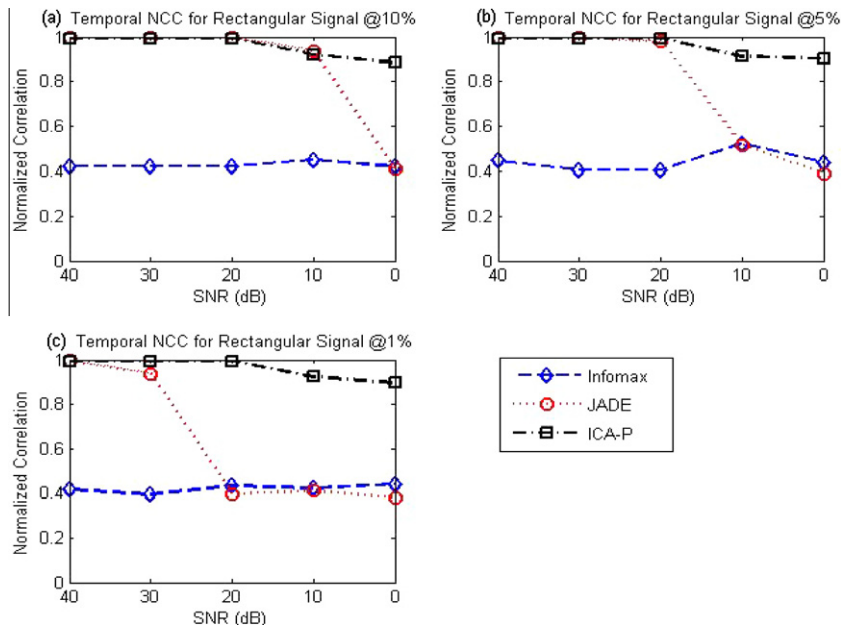


Fig. 3. Temporal NCC results for the rectangular signal on synthetically-generated video.

$$\text{SBR (dB)} = 10 \log_{10} \frac{\sigma_S^2}{\sigma_B^2} \quad (6)$$

where σ_S^2 is the variance of the functional signal and σ_B^2 is the variance of the background.

Five videos were synthesized starting with the SBR ranging from 0 dB to -40 dB at -10 dB intervals. The amplitude of the sig-

nal is directly proportional to the level of SBR. A 0 dB SBR indicates that the variance of the functional signal is equal to the variance of the video, whereas a -30 dB SBR means that the variance of the functional signal is 0.1% of the variance of the video. As mentioned before, the main objective of these experiments is to determine the lowest amount of variation of the signal that can be detected by the ICA and ICA-P algorithms because in the future we will need to per-

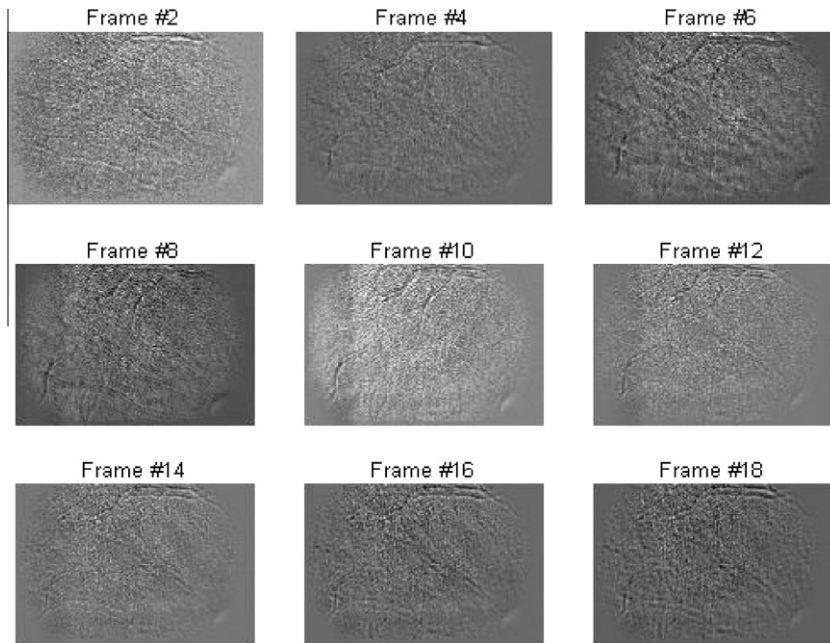


Fig. 4. Live data with simulated stimulus frames for -20 dB SBR. A vertical bar stimulation can be seen starting on frame #6 and continuing until frame #14.

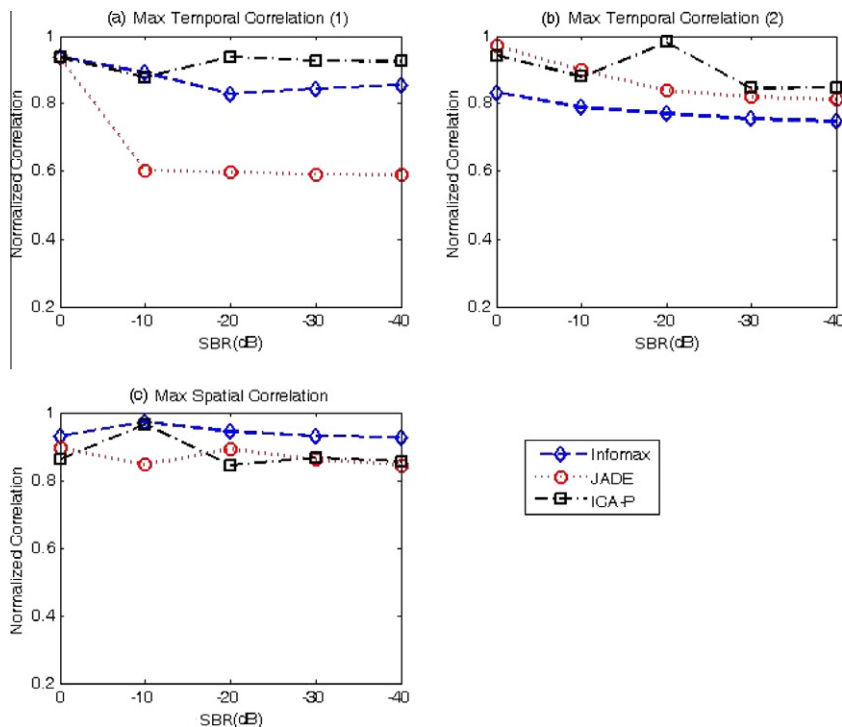


Fig. 5. Temporal and spatial correlation results for live data plus synthetic stimulation experiments. (a) Temporal correlation results using the temporal reference 1. (b) Temporal correlation results using the temporal reference 2. (c) Spatial correlation results using the reference frame.

form experiments on human retinas, which have functional responses to visual stimulation that are one order of magnitude lower than those measured on cat's retinas.

The results of the ICA-P and ICA algorithms were compared in the temporal and spatial domains. The spatial domain comparison was done by correlating the sources as estimated by each algorithm with a “reference frame,” which is an image artificially generated by using a frame of pre-stimulated retina and the artificial stimulus. For the temporal comparison, each row of the estimated mixing matrix \hat{A} was correlated with the two expected simulated functional responses, one with a negative response to the visual stimulation due to functional changes, and the other with a positive response due to blood flow increase. These two responses have been shown to have different delays with respect to the visual stimulation. The positive response due to increase in blood flow is noticed as soon as the stimulus starts, while the functional response peaks about 3 s after the visual stimulation is started.

Fig. 5 shows the maximum absolute correlation values at zero lag for (a) temporal reference #1, i.e. the blood flow response as measured in the bright area of the retina, (b) temporal reference signal #2, i.e. the functional response as measured in the dark area of the retina, and (c) reference frame. Increased NCC values are observed in the temporal cases (Fig. 5a and b) and a minor decrease compared to the Infomax in the spatial case (Fig. 5c).

4. In vivo cat data analysis

The data set selected for the cat data analysis consists of 60 videos with four different types of stimulation. All the videos (epoch) have a duration of 10 s (s), with a frame rate of two frames per second (fps). The stimulus paradigm consists of a checkered pattern with alternating polarity that is off for the first 2 s, representing the baseline (pre-stimulus), on for 3 s of stimulation, and off for 5 s of recovery (post-stimulus). The stimulus is applied in different spatial regions at multiple orientations. Our data is composed of 18 videos with vertical bar stimulation, 18 with horizontal bar stimulation, three with spot stimulation (The pattern is a small box), three with full field stimulation (the stimulus pattern covers the whole field of view) and 18 with no stimulation (for control purposes) for a total of 60 videos.

The videos were processed using ICA-P, Infomax, and first frame analysis (FFA). FFA is a simple video processing technique where the first frame of the sequence is removed from the remaining frames in the video. Comparison of the three methods is described below. Here, we do not report results from JADE since it produced similar results as Infomax, as seen in Barriga et al. (2007).

When comparing the results of ICA-P with traditional analysis such as FFA, we note a slight increase in the contrast of the detected signal (Fig. 6a and b). As expected, a more compact temporal response is found using ICA-P (Fig. 6c). We note that traditional analysis is performed manually, having to identify the areas of suspected activity and then extracting the temporal response by selecting a region of interest.

The introduction of the ICA-P algorithm allows us to visualize the functional signals for a variety of confidence and tolerance values. It is interesting to note from the synthetic simulations that in several examples, different combinations of confidence and tolerance values yielded very similar results. For the real data set, due to the lack of ground truth data, we are led to look for consistency in our signal detection results.

We present a successful signal detection example in Fig. 7. The original Infomax algorithm is shown in Fig. 7a. The time courses from two different confidence and tolerance values are shown in Fig. 7b and c. To normalize the detected signals, we first find the absolute maximum signal value and then divide all other samples

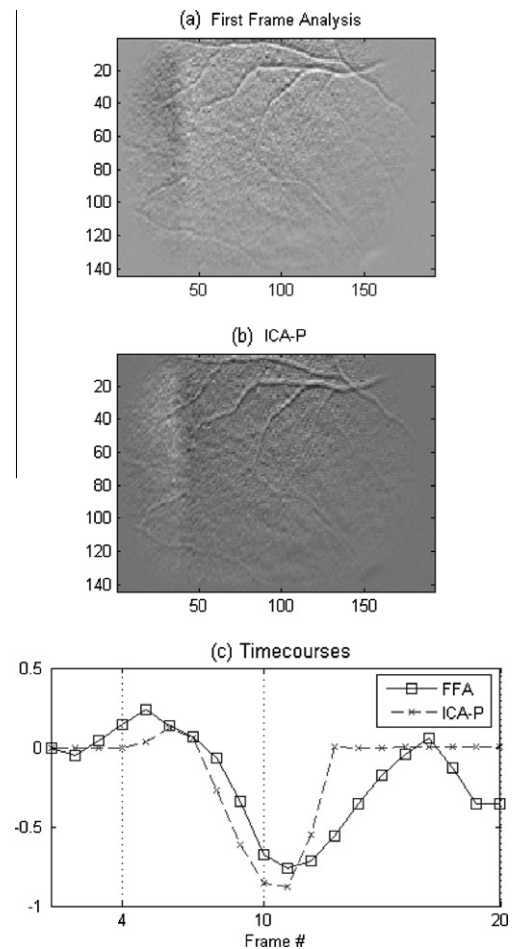


Fig. 6. (a) First frame analysis of a live cat data experiment #7 of 60. The frame shown is the one with the highest contrast in all the video. (b) Spatial result of applying ICA-P to the live cat data recording. (c) Temporal comparison of time courses found with FFA and ICA-P. The visual stimulus is applied between frames 4 and 10.

by it. As a result, all signals have -1 as their minimum value. As we see in Fig. 7a–c, the change due to visual stimulation can be extracted using any of the three algorithms. However, we also notice that Infomax show a “dark” response on top of a “bright” response, while the two ICA-P signals have these signals inverted. This is not uncommon among ICA algorithms, due to the uncertainty principle of ICA (Hyvarinen et al., 2001).

From the results in Fig. 7d, it is interesting to note that frame #10 consistently gave the location of the lowest reflectance value. This result is independent of the confidence parameter. We have observed this behavior consistently, in agreement with a visual inspection of the data sets. Beyond agreement in the minimum value, we also observe that the time-courses appear to cluster around some central time course. While there is strong variability within each cluster, it also appears that the time courses tend to oscillate around each other.

Fig. 8 shows the spatial profile of the functional response. We have noted that the region where the response to the stimulus is seen is formed by two adjacent regions, one brighter and the other darker than the rest of the image. We have noted variations of this phenomenon in all cat videos, but thus far there is not a satisfactory physiological explanation (Schallek et al. 2009a,b).

We present a typical example where no signal detection was possible in Fig. 9. The lack of any consistency in the results is very evident in Fig. 9d. There is no consistency in the location of the peak values. There is no evidence of clustering in the results either.

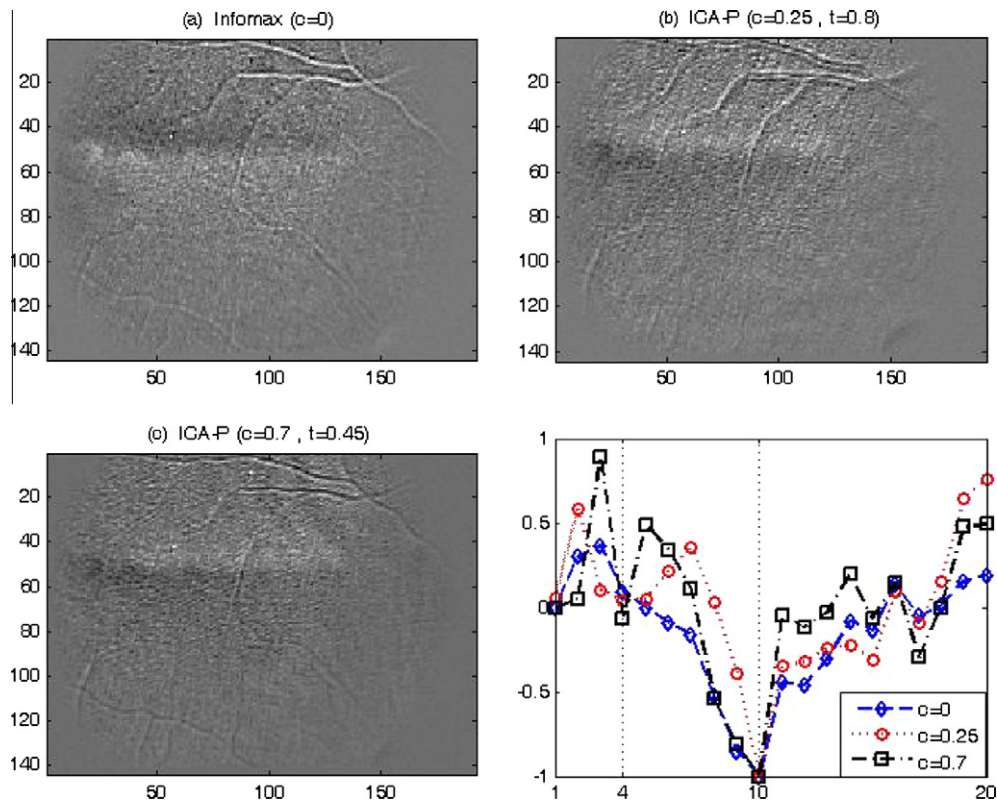


Fig. 7. Spatial (a–c) and temporal (d) signals extracted from an in vivo experiment #13 of 60 with horizontal visual stimulation.

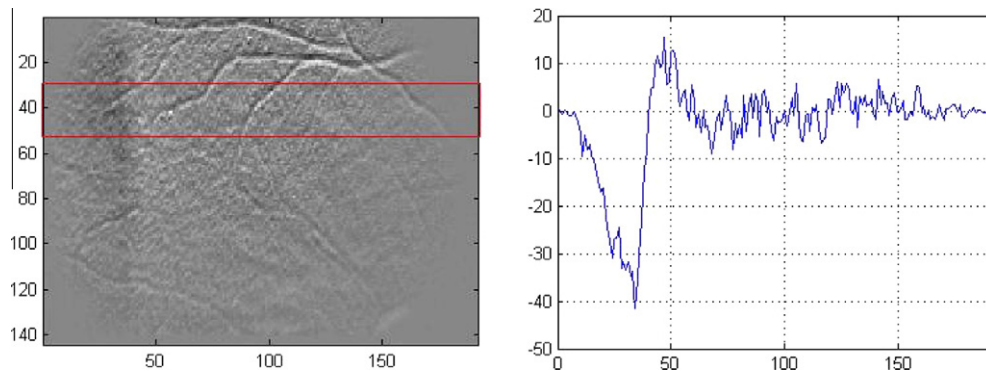


Fig. 8. Line intensity profile for a vertical stimulation experiment (video #7 of 60). The plot on the right corresponds to the average value in the X-direction from the red box in the ICA-P (extracted) image of the left.

The lack of any consistency suggests that the ICA-P algorithms converged to different signals.

Overall, both the current ICA-P and original Infomax method provided a detection rate of 86%. As outlined by Barriga et al. (2007), the results do agree with visual inspection. The consistency of the detected signals for a variety of ICA-P parameters also serves to increase our confidence in the detection results. In addition, the lack of responses found in experiments with no stimulation increases our confidence that the ICA-P algorithm does not add ghost signals from the priors.

5. Discussion and conclusions

The experiments presented in this paper have provided us with an improved understanding of the limits of what ICA-P and ICA algorithms can achieve to extract functional signals related to

BOLD responses, and how they can be improved. For the performance of ICA-P in the 3-dimensional simulations, we note significant improvement over conventional ICA algorithms.

The results of the temporal correlations for the synthetic video simulations (Fig. 3) showed that detection was possible at a SNR level of 0 dB as opposed to 30 dB for JADE (see discussion at the end of Section 3.1). The results on the hybrid simulations also showed an improvement in the temporal correlations of about 0.05 in absolute normalized cross-correlation. These results demonstrate the power of introducing prior information about the temporal structure of the experiments.

The application of ICA-P and ICA algorithms to live cat recordings has produced a success rate of 86% in the detection of the functional signals. The videos where no stimulation was detected corresponded to vertical and horizontal stimulation close to the edges of the field of view. Likely, these stimulus patterns did not stimulate enough area in the retina to produce a measurable re-

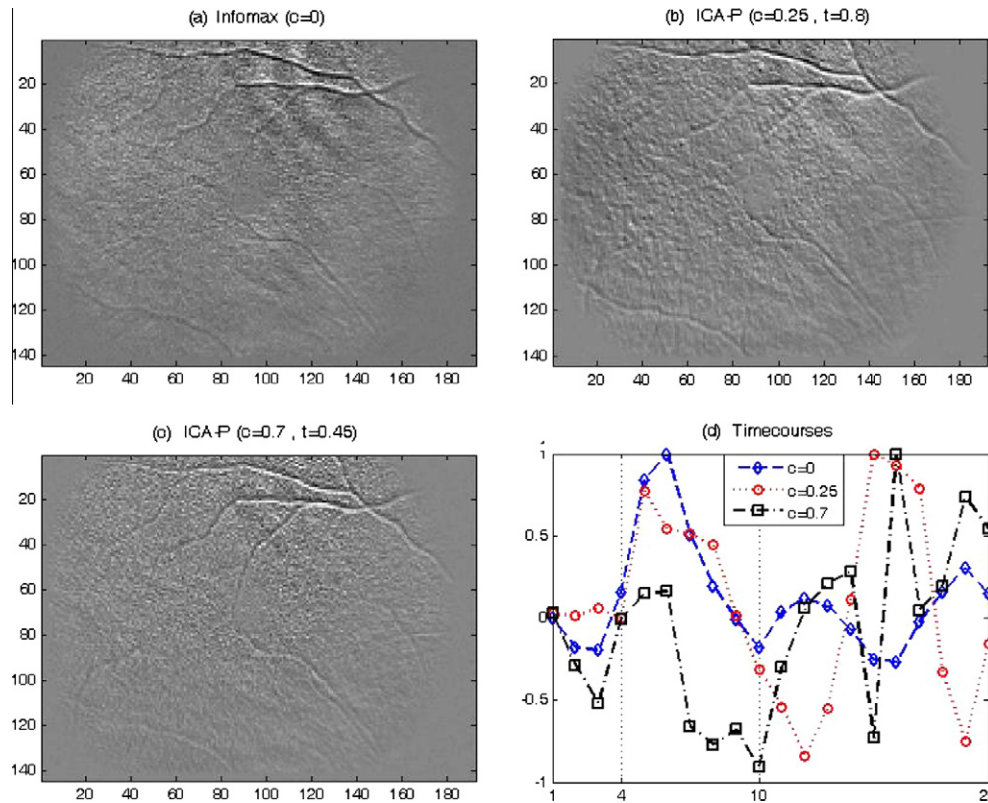


Fig. 9. Temporal and spatial signals extracted from an in vivo experiment where no response to visual stimulus was applied. Notice that there is no false detection of responses by the ICA algorithms.

sponse and thus were missed by all the detection algorithms. The results from the hybrid simulations show that we can estimate changes as small as 0.01% (−40 dB) of the total intensity levels in the images, which are at least two orders of magnitude lower than the ones that appear to be present in the live cat data recordings.

We observed strong consistency in our signal detection results for the cat videos. ICA-P results for difference confidence and tolerance parameters produced functional signals that produced the largest stimulated response at the same frame number, while exhibiting strong clustering characteristics. The consistency of the detected signals for a variety of ICA-P parameters also serves to increase our confidence in the detection results. In addition, the lack of responses found in experiments with no stimulation increases our confidence that the ICA-P algorithm does not add ghost signals from the priors.

We believe that a system like the one presented in this paper could find its way into the clinic, but more research is needed about the origins of the signals and the effects of the visual stimulation. In previous papers we have hypothesized that in a normal retina the functional responses could be seen regardless of the position of the visual stimulation. An abnormal retina would have areas of no response to the stimuli, and therefore a doctor could do an assessment of the functionality of the patient's retina in a more quantitative way and without depending on the cooperation of the patient.

Future work will be concentrated on automation of the confidence and tolerance parameters. We also intend to add spatial information on the priors, which at this point has not been possible due to the high-dimensionality of the problem.

In conclusion, significant improvement over the Infomax algorithm (which the ICA-P generalizes) has been achieved in the synthetic simulations based on physiological data. Moreover, the ICA-

P outperforms conventional ICA algorithms for up to 30 dB on simulated experiments, proving to be a powerful tool for the analysis of complex biological signals. In the problem of signal detection, the requirement was to estimate signals as small as 0.1% of the total intensity of the images, and we have achieved detection for signals as small as 0.01% (−40 dB SBR) in the hybrid data simulations.

References

- Abramoff, M.D., Kwon, Y.H., Ts'o, D., Soliz, P., Zimmerman, B., Pokorny, J., Kardon, R., 2006. Visual stimulus induced changes in human near-infrared fundus reflectance. *Investigative Ophthalmology and Visual Sciences (IOVS)* 47, 715–721.
- Barriga, E.S., Ts'o, D.Y., Pattichis, M.S., Soliz, P., 2003a. Independent component analysis for processing of retinal responses to patterned stimuli. In: *Engineering in Medicine and Biology Society, 2003. Proceedings of the 25th Annual International Conference of the IEEE*, vol. 1, pp. 1006–1009.
- Barriga, E.S., Truitt, P.W., Pattichis, M.S., Ts'o, D., Kwon, R.H., Kardon, R.H., Soliz, P., 2003b. Blind source separation in retinal videos. In: *Medical Imaging 2003: Image Processing. Proceedings of the SPIE* 5032, pp. 1591–1601.
- Barriga, E.S., Pattichis, M.S., Ts'o, D.Y., Kwon, Y., Kardon, R., Abramoff, M.D., Soliz, P., 2006. Detection of low amplitude, in-vivo intrinsic signals from an optical imager of retinal function. In: *Ophthalmic Technologies XVI. Proceedings of the SPIE* 6138, pp. 66–77.
- Barriga, E.S., Pattichis, M.P., Ts'o, D.Y., Abramoff, M., Kardon, R., Kwon, Y., Soliz, P., 2007. Spatiotemporal independent component analysis for the detection of functional responses in cat retinal images. *IEEE Transactions on Medical Imaging* 26, 1035–1045.
- Bell, A.J., Sejnowski, T.J., 1995. An information-maximization approach to blind separation and blind deconvolution. *Neural Computation* 7, 1003–1034.
- Calhoun, V.D., Adali, T., Stevens, M.C., Kiehl, K.A., Pekar, J.J., 2005. Semi-blind ICA of fMRI: a method for utilizing hypothesis-derived time courses in a spatial ICA analysis. *Neuroimage* 25, 527–538.
- Calhoun, V.D., Adali, T., 2006. Unmixing fMRI with independent component analysis. *IEEE Engineering in Medicine and Biology* 25, 79–90.
- Cardoso, J., 1997. Infomax and maximum likelihood for blind source separation. *IEEE Letters on Signal Processing* 4 (4), 112–114.

- Choi, S., Cichocki, A., Amari, S., 1999. Fetal electrocardiogram data analysis via flexible independent component analysis. Presented at the 4-th Asia-Pacific Conference on Medical & Biological Engineering (APCMBE'99), Seoul, Korea.
- Grinvald, A., Lieke, E., Frostig, R.D., Gilbert, C.D., Wiesel, T.N., 1986. Functional architecture of cortex revealed by optical imaging of intrinsic signals. *Nature* 324, 361–364.
- Hanazono, G., Tsunoda, K., Shinoda, K., Tsubota, K., Miyake, Y., Tanifuji, M., 2007. Intrinsic signal imaging in macaque retina reveals different types of flash-induced light reflectance changes of different origins. *Investigative Ophthalmology and Visual Science (IOVS)* 48, 2903–2912.
- Hare, W.A., Ton, H., 2002. Effects of APB, PDA, and TTX on ERG responses recorded using both multifocal and conventional methods in monkey. *Documenta Ophthalmologica* 105, 189–222.
- Hill, D.K., Keynes, R.D., 1949. Opacity changes in stimulated nerve. *Journal of Physiology* 108, 278–281.
- Hofmann, K.P., Uhl, R., Hoffmann, W., Kreutz, W., 1976. Biophysics of Structure and Mechanism 2, 61–77.
- Hyvarinen, A., Karhunen, J., Oja, E., 2001. *Independent Component Analysis*. John Wiley, New York.
- Jung, T.-P., Humphries, C., Lee, T.-W., McKeown, M.J., Iragui, V., Makeig, S., Sejnowski, T.J., 2000. Removing electroencephalographic artifacts by blind source separation. *Psychophysiology* 37, 163–178.
- Juslin, Anu, Reilhac, Anthonin, Magadan-Mendez, Margarita, Alban, Edisson, Tohka, Jussi, Ruotsalainen, Ulla, 2005. Assessment of Separation of Functional Components with ICA from Dynamic Cardiac Perfusion PET Phantom Images for Volume Extraction with Deformable Surface Models. FIMH 2005, LNCS 3504, pp. 338–347.
- Kahlert, M., Pepperberg, D.R., Hofmann, K.P., 1990. Effect of bleached rhodopsin on signal amplification in rod visual receptors. *Nature* 345, 537–539.
- Kardon, R., Kwon, Y.H., Truitt, P.W., Nemeth, S.C., Ts'o, D., Soliz, P., 2002. Optical imaging device of retinal function. In: *Ophthalmic Technologies XII*. Proceedings of the SPIE, vol. 4611, pp. 230–238.
- Liao, Rui, Krolik, J.L., McKeown, M.J., 2005. An information-theoretic criterion for intrasubject alignment of fMRI time series: motion corrected independent component analysis. *IEEE Transactions on Medical Imaging* 24 (1), 29–44.
- Makeig, S., Bell, A.J., Jung, T.-P., Sejnowski, T.J., 1996. *Independent component analysis of electroencephalographic data*. In: *Advances in Neural Information Processing Systems*. MIT Press, Cambridge, MA, pp. 145–151.
- McKeown, M.J., Sejnowski, T.J., 1998. Independent component analysis of fMRI data: examining the assumptions. *Human Brain Mapping* 5, 368–372.
- Milles, Julien, van der Geest, Rob J., Jerosch-Herold, Michael, Reiber, Johan H.C., Lelieveldt, Boudewijn P.F., 2008. Fully automated motion correction in first-pass myocardial perfusion MR image sequences. *IEEE Transactions on Medical Imaging* 27 (12), 1812–1836.
- Nelson, D.A., Krupsky, S., Pollack, A., Aloni, E., Belkin, M., Vanzetta, I., Rosner, M., Grinvald, A., 2005. Special report: noninvasive multi-parameter functional optical imaging of the eye. *Ophthalmic Surgery, Lasers & Imaging* 36, 57–66.
- Park, S.-J., An, K.-H., Lee, M., 2002. Saliency map model with adaptive masking based on independent component analysis. *Neurocomputing* 49, 417–422.
- Schallek, J.B., Kardon, R.H., Kwon, Y.H., Abramoff, M.D., Soliz, P., Ts'o, D., 2009a. Stimulus-evoked intrinsic optical signals in the retina: pharmacological dissection reveals outer retinal origins. *Investigative Ophthalmology and Visual Science* 50, 4865–4872.
- Schallek, J.B., Li, H., Kardon, R.H., Kwon, Y.H., Abramoff, M.D., Soliz, P., Ts'o, D.Y., 2009b. Stimulus-evoked intrinsic optical signals in the retina: spatial and temporal characteristics. *Investigative Ophthalmology and Visual Science* 50, 4873–4880.
- Schiessl, I., Stetter, M., Mayhew, J.E.W., McLoughlin, N., Lund, J.S., Obermayer, K., 2000. Blind signal separation from optical imaging recordings with extended spatial decorrelation. *IEEE Transactions on Biomedical Engineering* 47, 573–577.
- Slaughter, M., Miller, R., 1983. An excitatory amino acid antagonist blocks cone input to sign-conserving second-order retinal neurons. *Science* 219, 1230–1232.
- Stepnoski, R.A., LaPorta, A., Racchia-Behling, F., Blonder, G.E., Slusher, R.E., Kleinfeld, D., 1991. Noninvasive detection of changes in membrane potential in cultured neurons by light scattering. *Proceedings of the National Academy of Sciences of the United States of America* 88, 9382–9386.
- Stetter, M., Schiessl, I., Otto, T., Sengpiel, F., Hübener, M., Bonhoeffer, T., Obermayer, K., 2000. Principal component analysis and blind separation of sources for optical imaging of intrinsic signals. *Neuroimage* 11, 482–490.
- Ts'o, D.Y., Li, H., Kwon, Y.H., Truitt, P., Soliz, P., 2003. Intrinsic signal optical imaging of retinal responses to patterned stimuli. *Investigative Ophthalmology and Visual Sciences (IOVS)* 44, 2709.
- Ts'o, D.Y., Zarella, M., Schallek, J., Kwon, Y., Kardon, R., Soliz, P., 2004. The origins of stimulus dependent intrinsic optical signals of the retina. *Journal of Vision* 4, 39.
- Ts'o, D.Y., Schallek, J.B., Kardon, R., Kwon, Y., Abramoff, M., Soliz, P., 2009. Hemodynamic components contribute to intrinsic signals of the retina and optic disc. *Investigative Ophthalmology and Visual Science* 50 (E-Abstract 4322).
- Tsunoda, K., Oguchi, Y., Hanazono, G., Tanifuji, M., 2004. Mapping cone- and rod-induced retinal responsiveness in macaque retina by optical imaging. *Investigative Ophthalmology and Visual Science (IOVS)* 45, 3820–3826.
- Villringer, A., Chance, B., 1997. Noninvasive optical spectroscopy and imaging of human brain function. *Trends in Neuroscience*, 435–442.
- Yao, X.C., George, J.S., 2006. Dynamic neuroimaging of retinal light responses using fast intrinsic optical signals. *Neuroimage* 33, 898–906.